



Prognostication of Kimberlites in Parts of Eastern Dharwar Craton: Inferences Through Aeromagnetic Signatures

KEYWORDS

Prognostication, Kimberlite emplacement, structural configuration, high resolution Airbornemagnetic survey, Deconvolution.

A.Subhash Babu

G. Ramadass

M. Preeti

RMSI Private Limited, Hyderabad.

Center for Exploration Geophysics,
Osmania University, Hyderabad.

Center for Exploration Geophysics,
Osmania University, Hyderabad.

ABSTRACT Aeromagnetic data, covering 1999 Sq.km of Mahabubnagerand Gulbarga districts of Telangana and Karnataka states in the Eastern Dharwarcraton,India to evaluate the structural configuration of the region. From IGRF corrected magnetic data,RTP(Reduction to pole), Horizontal (X and Y direction), Vertical and Total (analytical signal) gradient maps, several lineaments trending in three major directions NE-SW, NW-SE and E-W were identified. The Zones of intersection of these structural trends which could have acted as potential sites for kimberlites emplacement were accordingly delineated at 21 locations (AA1,BB1to BB5,CC1 to CC2,DD1toDD2, EE1, FF1, GG1to GG3,HH1to HH3 and II1).

We calculated depth of prognosticatedkimberlitezones through Euler Deconvolution and Power spectrummethods and magnetic interface in the region was obtained using GM-Sys Inversion modeling of 21 profiles.The inferred magnetic interface is exhibiting V-shaped/ caret type structure.

Introduction

An aeromagnetic survey is the most economical method of understanding a geophysical reconnaissance of any relatively unexplored or inaccessible region. It provides data on a broad scale of structural trends, the position of faults and the distribution of shallow or deep crystalline basement as well as the occurrence of volcanic rocks within a sedimentary basin. A national Program of aeromagnetic survey was organized by the Geological survey of India (GSI) to cover the entire country by systematic Multi-sensor Twin Otter aero geophysical surveys were carried out by AMSE wing of GSI During 2001-04, about 12,940 sq km was flown at 500 m line spacing and 150 m flight altitude in Nalgonda, Mahabubnagar and Narayanpet areas in Telangana.

Aeromagnetic lineaments are usually identified with faults and geological structural trends. All the magnetic lineaments are not alike. A proper classification of these lineaments reveals a wealth of structural detail. Therefore, Geophysical detection of kimberlite and related rocks involving contrasts in physical properties such as magnetic susceptibility contrasts between kimberlites and their host rocks has been used (Macnae,1995, and Power et al, 2004) Several studies have been reported over the study region and few academic publications were available on theNarayanpetKimberlite Field (NKF) are restricted to Narayanpet, Maddur and Kotakota areas. About BhimaKimberlite Field, published literature is scanty. Some of the authors (Sreerama Murthy et al.1997, 1999, Ramadass et al.2004a, 2004b, 2006a & 2006b, Veeraiiah 2004, Veeraiiah et al. 2006& 2009, Mallick et al. 2012) through some light on adjacent areas.

Thestudy area is well known for the occurrence of kimberlites are located in the Eastern Dharwarcraton (EDC) of south India. An attempt is made here to infer magnetic interface and to obtain a clearer perception of the structural configuration and to find any possible correlation between thekimberlites occurrences using high resolution aeromagnetic data in parts of Mahabubnagar district of

Telangana State and parts of Gulbarga district of Karnataka State, India.

Geology and Tectonics

Geologically, its character is typical falling under Archean-Precambrian EasternDharwarcraton.TheDharwarcraton is considered to consist of two distinct geological sub-cratons, the older western Dharwarcraton and the eastern Dharwarcraton (Rajamani1990). The Narayanpet region is characterized by crustal deformation and forms a type area for the eastern sub-craton (Ramadass et al 2006). Where theleocoitic and komatiitic meta- basalts and felsic volcanic formed 2700 million years ago (Balaskirhnan et al 1990,Krogstad et al 1989).The area mainly consists of granite gneiss and granitoids suites of rocks of Archean age associated with older metamorphic/metobasites, name ly,pyroxenites,amphibolites, bitotiteschists, migmatites and basid dykes of doleritic and gabbroic composition. A number ofNW-SE, E-W and NE-SW trending intrusive dykes are a geologically distinctive feature of the area.

The geology of Narayanpet areashown in Figure 1. (GSI,2011), north of Krishna River is represented by grey granite and gneiss with minor pink feldspar bands representing the Peninsular Gneissic Complex (PGC). The zone east of Yadgir is marked by metabasicschists and amphibolites bands within the PGC as basic enclaves Narayanpet-Kimberlite Field (NKF) is characterized by two main fracture domains: an E-W trending strike slip fault associated NE-SW trending fractures in the Maddur-Kotakonda area, and a predominantly E-W trending strike-slip fault set with associated NNW-SSE trending fractures west of Narayanpet. All the known kimberlites of the NKF are located either along the E-W trending faults or at their intersection with the NNW-SSE trending or NE-SW trending fractures (Rao et al. 1998). All the kimberlites of NKF are emplaced into migmatitic gneisses, and granitoids.

Data Base

High resolution Aero-magnetic data procured from Airborne Mineral Surveys and Exploration (AMSE) division of

Geological Survey of India (GSI). The surveys conducted by various nodal agencies are mosaicked seamlessly and supplying in IGRF corrected contour map formats. The agencies involved in the multi-sensor air-borne data acquisition were mainly OHR, BRGM-CGG, NGRI, NRSA, GSI and AMD. The current study area was covered by Twin Otter Airborne Survey System (TOASS) by GSI in 2000-2001 about 12,940sq.km. Aeromagnetic (GSI 2013) from the study area lies in-between geographic coordinates of 16° 50' 25"N, 77° 04' 41"E and 16° 29' 39"N, 77° 35' 26"E and falls in parts of the Survey of India (SOI) 1:50,000 scale top-sheets of 56 H1,2,3,5,6,7,9,10 and 11, collected in the period 2000-2001 with NE-SW oriented flight lines direction and clearance of 120m(AGL), 500m mean flight line spacing, Contour Interval 10nT Mean Inclination 19.33° Mean Declination -1.353° and Mean Total Field of 41528.9nT IGRF corrected data in the scale of 1:50,000 purchased from Airborne mineral Surveys and Exploration wing (AMSE) of GSI.

Qualitative Analysis

Figure 2 is the contoured IGRF corrected Total Magnetic Intensity of the study area, contoured with an interval of 10nT. The magnetic signatures range from a low of -150nT along western region of the study area, to a high of 550nT in the south-western and north-eastern parts of the region. From these figures, the high magnetic trend is almost near the confluence of Krishna and Bhimarivers as well as north-eastern highlands (north of Narayanpet town). While in the colour contoured map, variation in the absolute field, inclination and declination are shown respectively.

Figure 2 shows the distinct pattern of highs and lows. At some places steep gradients between them are described as prominent magnetic lineaments. Which are attributable to the complex assemblage of features of varied dimensions and directions from different phases of magmatic activity. Some of the features are associated with basic/ultra basic/younger acidic intrusives that indicate zones of magnetic permeability (Sinha et al. 2003).

While comparison of the magnetic signatures with geology of the region not many inferences are made because the various forms of granites (migmatites, gneisses, pink/ grey granites and/or biotite granites) are magnetically not much distinctive. The magnetic highs and lows are in conjunction of subsurface faults in the granitic terrain. Not with the composition of the granites, the study area covers various forms of granites along with little Dharwar schist. Few basic/ ultra basic dykes are available as intrusive rocks. A NW-SE trend to NE-SW trends of fault axes are evident in highs and lows in figure.3 Two other trends of magnetic high responses are also running in the same direction.

Interesting features observed in this area are intersections of various magnetic linear features which are supposed to be intersection of faults. These features are prognosticated kimberlite emplacement at 21 places (AA1, BB1 to BB5, CC1 to CC2, DD1 to DD2, EE1, FF1, GG1 to GG3, HH1 to HH3 and II1) in the study region shown in Figure 3.

Reduction to Pole (RTP)

The shape of a magnetic anomaly depends on the shape of the causative body. But unlike a gravity anomaly, a magnetic anomaly also depends on the inclination and declination of the body's magnetization, the inclination and declination of the local earth's magnetic field, and the orientation of the body with respect to magnetic north. To simplify anomaly shape, Baranov (1957) and Baranov and

Naudy (1964) proposed a mathematical approach known as reduction to the pole. This method transforms the observed magnetic anomaly into the anomaly that would have been measured if the magnetization and ambient field were both vertical — as if the measurements were made at the magnetic pole. This method requires knowledge of the direction of magnetization, often assumed to be parallel to the ambient field, as would be the case if remnant magnetization is either negligible or aligned parallel to the ambient field. The computed reduced to pole values of the study area is shown in Figure.4.

Horizontal, Vertical and Total (Analytical) gradients

Gradient maps help define geological contacts more sharply contour maps as also give an estimate of the depth of the source body and the location and dip of its edges. Horizontal gradients of magnetic anomalies are clearly noticed over edges of tabular bodies. For near surface bodies with near-vertical contacts, the maximum horizontal gradient of magnetic as measured along the profile will occur nearly over the contact (Dobrin and Svit, 1988).

The horizontal gradient along the X and Y directions shown in Figures 5 and 6, represent the rate of change of the magnetic field in the corresponding directions that is: the X - gradient highlights anomalies with large components disposed along the Y-axis and vice-versa. However, in the study region shows varying trends NW-SE, NE-SW and E-W.

Vertical derivatives, on the other hand are based on the concept that the rate of change of magnetic field is much more sensitive to demarcation of geological boundaries, details of which are obscured in the original map. Figure 7 is a plot of the vertical derivative of the total magnetic intensity of the study region. This map is dominated by essentially NW-SE and NE-SW striking anomalies. Most of the high frequency anomalies seen in the vertical derivative map.

The analytical signal (Total gradient) Figures 8 gives finer resolutions of magnetic anomaly trends and locations and disposition of causatives (Ramadas et al 1990) the anomaly square root of the (Nabighain, 1972) sum of squares of the horizontal (X and Y) and vertical derivatives (Z) along the orthogonal axes of the anomaly resolves the anomaly map — it encompasses information of the magnetic field variation along the orthogonal axes completely defining it. Consequently, structural features and boundaries of causative sources can be determined more accurately.

From the analytical signal map of the aeromagnetic in the signal shaded anomaly map of study area is represented in Figure 8 of the study region is reflecting similar trends observed in total magnetic intensity map, which suggests that the magnetic basement occurs at shallow depth.

Quantitative Analysis

The purpose of quantitative analysis of magnetic data in the study area was to obtain the subsurface configuration of the magnetic interface in the study region, quantitative analysis was attempted.

Though there are many ways to attempt quantitative estimates of depth to an intracrustal magnetic interface. Therefore, in the present studies Peter's half slope method. Modeling / Inversion, spectral method and Euler deconvol-

lution methods were performed on 21 profiles from AA1, BB1 to BB5, CC1 to CC2, DD1 to DD2, EE1, FF1 to FF3, GG1 to GG3, HH1 to HH3 and II of length of up to 10 KM (Figure.9).

Depth of the prognosticated kimberlite areas are calculated through Euler Devolution Method. Profiles AA1, BB1 to BB5, CC1 to CC2, DD1 to DD2, EE1, FF1 to FF3, GG1 to GG3, HH1 to HH3 and II1 are generated for these prognosticated areas to calculate the same (Figure.10.1 to 10.3) and cross-correlated with profile models (Table 1).

In the current study Fast Fourier Transform (FFT) filter is used to calculate the depth. The data is transformed from the space domain to the wavenumber domain using an FFT. The wavenumber increment of the resulting transform will be $1/(\text{line-length})$.

The power spectrum of the aeromagnetic gives an idea of the distribution of magnetic sources at different depth levels. The shallow levels being represented by high frequency part of the spectrum while deeper or regional levels are reflected in the low frequency part of the spectrum (Spector and Grant, 1970).

Vertical derivatives (Blakely, 1995) of the potential fields amplify short wavelength information at the expense of long wavelength information and thus help to resolve shallow sources. Depth of the prognosticated kimberlite locations are calculated through radially averaged Power Spectrum Method. Profiles AA1, BB1 to BB5, CC1 to CC2, DD1 to DD2, EE1, FF1 to FF3, GG1 to GG3, HH1 to HH3 and II1 (Figures 11.1 to 11.3) are generated for these prognosticated areas to calculate the same shown in (Table.1).

Inversion/Modeling

The software used for inversion is the GM-SYS (2000), a magnetic modeling software from Northwest Geophysical Associates Inc. This software is based on the methods of Talwani et al. (1959). Talwani and Heritzler (1964) make use of the algorithms described in Won and Bevis (1987). The software assumes a two dimensional flat earth model and uses the USGS SKI (Webring, 1985) implementation of the Margaret inversion algorithm (Margaret, 1963) to linearize and invert the calculation.

The observed and computed fit of the anomaly as also the inferred magnetic interface along the profiles modeled assuming a two layer (upper and lower magnetic layer based on the magnetic lineament trend) are shown in profiles of AA1, BB1 to BB5, CC1 to CC2, DD1 to DD2, EE1, FF1 to FF3, GG1 to GG3, HH1 to HH3 and II1. For the present investigation a uniform low/high average magnetic susceptibilities of 0.005 cgs obtain from different workers (Ramadass et al. 2007) and a remanance of on 0.00175 were assumed for the magnetic layer of the crust. The magnetic inclination and declination for the area taken to be 19.33° and -1.33° respectively.

From modeled body, magnetic basement layer along these profiles are less than 300 meters all along except at centre of the anomaly. The increase in depth of magnetic basement probably showing the intrusion type bodies.

Profile AA1

This profile is situated west of Yadgir town and estimated depth 600, 684, 664 and 759 m depth as per the Half-Slope, Power Spectrum (Figure 11.1.(a)) and Euler deconvolution methods. This is at the intersection of NNW-SSE

and E-W (almost) faults. The maximum magnetic response along this profile exhibits 140nT. The inferred magnetic interface is less than 12989 m and width at the centre is 250 m, exhibiting the caret type structure, suggest the presence of kimberlitic body (Figure 10.1.(a)).

Profiles BB1 to BB5

These profiles are running almost NW-SE to E-W and again NW-SE from north of Yadgir town to east of Utkur village almost at a length of 55 km. Total 5 kimberlite pipes are prognosticated in this section. The depths of BB1 to BB4 are about 505 to 855 m, where as the BB5 is almost 1700 m depth as per the Half-Slope, Power Spectrum (Figures 11.1.(b) to 11.1.(f)) and Euler deconvolution methods. BB1 and BB2 inferred magnetic interfaces are ranging from 8702 m to 13379 except BB3, which is 3330 m and in the centre 200-300 m width, exhibiting the caret type structure; suggest the presence of kimberlitic bodies. BB3 inferred magnetic layer is showing two kimberlite bodies with less than 10 km (left) and almost 5 km (right) with nearly 1000 m width. BB4 and BB5 inferred magnetic layers are nearly 10 km with nearly 2000 m width and looks like broad v shaped kimberlites. The maximum magnetic response along this profile exhibits 310nT and the minimum response along the fault line is 110nT (Figures 10.1.(b) to 11.0.(f)).

Profiles CC1 and CC2

These profiles are running E-W and then NE-SW at north-east corner of the study area. In between these two kimberlites many kimberlite pipes were identified by various authors and published by GSI. These two profiles are connected with magnetic highs in first vertical derivative image. The depths of CC1 are about 608 to 755 m, where as the CC2 is 824 to 10573 m as per the Half-Slope, Power Spectrum (Figures 11.1.(g) to 11.1.(h)) and Euler deconvolution methods. CC1 and CC2 inferred magnetic interfaces are 8881 m and 9727 m respectively and in the centre 1500 m width, exhibiting broad v shaped structure; suggest the presence of kimberlitic bodies. The maximum magnetic response along this profile exhibits 340nT and the minimum response along the fault line is 260nT (Figures 10.1.(g) to 11.0.(h)).

Profiles DD1 and DD2

These profiles are running E-W and running north of Narayanpet town. In between these two kimberlites many kimberlite pipes were identified by various authors and published by GSI. These two profiles are connected with magnetic highs in first vertical derivative image. The depths of DD1 and DD2 are about 469 to 660 m as per the Half-Slope, Power Spectrum (Figures 11.2.(i) to 11.2.(j)) and Euler deconvolution methods. DD1 and DD2 inferred magnetic interfaces are 12214 m and 9068 m respectively and in the centre 1500 m and 250 m width respectively. DD1 exhibiting broad v shaped structure; suggest the presence of kimberlitic bodies. Another small v shaped kimberlite pipe structure also seen in DD1. DD2 exhibiting the caret type structure, suggest the presence of kimberlitic body. The maximum magnetic response along this profile exhibits 270nT and the minimum response along the fault line is 220nT (Figures 10.2.(i) to 10.2.(j)).

Profile EE1

This profile is situated at southwest of Narayanpet town and almost 1130 to 1220 m depth as per the Half-Slope, Power Spectrum (Figure 11.2.(k)) and Euler deconvolution methods. This is at the intersection of NNW-SSE and NW-SE (almost) faults. The maximum magnetic response along

this profile exhibits 310nT. The inferred magnetic interface is 11850 m and the centre 1250 m width, exhibiting the broad v shaped structure; suggest the presence of kimberlitic body (Figure 10.2(k)).

Profiles FF1 to FF3

These profiles are running almost WSW-ENE south of Yadgir town. Total 3 kimberlite pipes are prognosticated in this section. The depths of FF1 to FF3 are about 446 to 765 m as per the Half-Slope, Power Spectrum (Figures 11.2.(l) to 11.2.(n)) and Euler deconvolution methods. FF1 and FF2 inferred magnetic interfaces are ranging from 10049 m and 8132 respectively and in the centre 300-400 m width, exhibiting the slightly broad v shaped structure; suggest the presence of kimberlitic bodies. FF3 inferred magnetic interface is 6683 m and with nearly 500 m width, exhibiting the caret type structure, suggest the presence of kimberlitic body. The maximum magnetic response along this profile exhibits 130nT and the minimum response along the fault line is -20nT (Figures 10.2.(l) to 10.2.(n)).

Profiles GG1 to GG3

These profiles are running in WSW-ENE north of Narayanpet Road Railway Station parallel to FF1 to FF3. Total 3 kimberlite pipes are prognosticated in this section. The depths of GG1 to GG3 are about 820 to 1107 m as per the Half-Slope, Power Spectrum (Figures 11.3.(o) to 11.3.(q)) and Euler deconvolution methods. GG1 and GG2 inferred magnetic interfaces are 15306 m and 9122 m respectively and in the centre 2000-2500 m width, exhibiting the broad v shaped structure; suggest the presence of kimberlitic bodies. GG3 inferred magnetic interface is 8401 m and with nearly 400 m width, exhibiting the caret type structure, suggest the presence of kimberlitic body. The maximum magnetic response along this profile exhibits 240nT and the minimum response along the fault line is 100nT (Figures 10.3.(o) to 10.3.(q)).

Profiles HH1 to HH3

These profiles are running in the direction of E-W parallel to 5 km north of southern border of the study area. Total 3 kimberlite pipes are prognosticated in this section. The depths of HH1 and HH3 are about 1220 to 1470 m as per the Half-Slope, Power Spectrum (Figures 11.3.(r) to 11.3.(t)) and Euler deconvolution methods. HH1 and HH3 inferred magnetic interfaces are 9166 m and 5192 m respectively and in the centre 2000-2500 m width, exhibiting the very broad v shaped structure; suggest the presence of kimberlitic bodies. HH2 inferred magnetic interface is 5192 m and with nearly 250 m width, exhibiting the caret type structure, suggest the presence of kimberlitic body. The maximum magnetic response along this profile exhibits 440nT and the minimum response along the fault line is 100nT (Figures 10.3.(r) to 10.3.(t)).

Profile II1

This profile is situated west of Narayanpet Road Railway Station and east of Wadgira village and almost 484 to 538 m depth as per the Half-Slope, Power Spectrum (Figures 11.3.(u)) and Euler deconvolution methods. This is at the intersection of NW-SE and E-W (almost) faults. The maximum magnetic response along this profile exhibits 320nT. The inferred magnetic interface is 10957 m and in the centre 400 m width, exhibiting the caret type structure, suggest the presence of kimberlitic body (Figures 10.3.(u)).

Discussion

A qualitative analysis of aeromagnetic data like reduction to Pole (RTP), Analytical signal. Derivative analysis (vertical

and Horizontal X and Y direction) has been performed to anticipate the subsurface structures and rock assemblages, where kimberlitic emplacement could be possible. Several magnetic lineament features suggesting the presence of various geological lineaments (Figure 2, 3 and 4). Thus lineaments that fall within the migmatite gneisses show a concordance relation with the regional Dharwarian trend, i.e., NW-SE, where as lineaments that fall over the biotite granites show both parallel as well as transverse relation, i.e., NW-SE, WNW-ESE, E-W, ENE-WSW and N-S trends. Intersecting lineaments form structural locales conducive for emplacement of kimberlites. The region around Maddur, a rich kimberlite field (Nayak Kasiviswanatham, 1988, Babu Rao et al. 1992, Sreerama Murty et al. 1997, 1999) is characterized by intersection of a few major and several minor tectonic elements.

Several lineaments criss-crossing and trending in two main directions, NW-SE and E-W are identified. Rao (1996) opines that the regional trend of kimberlite rocks in the Dharwar craton is possibly related to crustal warping and closely related deeply penetrating faults. It is evident that the inferred lineaments are associated with crustal deformation in the region.

Many studies on kimberlites have shown that the pre-requisites for the emplacement of kimberlites are (Woodzick and McCallum, 1984, Janse, 1992)

An ancient stable craton underlain by thick, cool and rigid continental lithosphere.

Deep reaching faults/ fractures.

Cross-cutting major structural trends.

Major cross structural trends in ancient cratons form the loci of kimberlite emplacement. In the present context, the two known kimberlite fields, viz., the WKF and the NKF occur in the granite-greenstone terrain of the eastern block of the Dharwar Craton. A close examination of the structural aspects vis-à-vis the distribution and disposition of the kimberlite bodies in the two known fields revealed that they are associated with an E-W trending strike slip faults with associated NE-SW resultant fractures domain in Maddur-Kotakonda area and a predominantly NNW-SSE trending and also E-W strike slip. All the known kimberlites of the NKF are located wither along the E-W faults or at their intersection with the NNW-SSE faults (Rao et al. 1998).

Kimberlite pipes generally occur as clusters. Most kimberlite clusters have an average diameter of about 40 km (Janse, 1985) while each individual cluster is composed of 1-20 distinct intrusions in close proximity (< 1 km) and separated by 2 km or more from other clusters (Mitchell, 1986). However, their prognostication is generally guided by investigating the structural controls which provide the necessary channels and locales for upwelling magma and emplacement of kimberlites. Various models for the occurrence of kimberlites have been proposed. Haggerty (1999) opined that they occur mainly as intrusions into Archaean and Proterozoic crust. Sykes (1978) and Haggerty, (1994) opined that while they originate in the mantle, reactivated fault/fracture systems control their intrusion into the crust.

Sreerama Murty et al. (1999) observed the association of kimberlites with large scale structural features like deep seated fault/ fracture corridors, domal structures, disjunctive zones of radial fractures, linear grabens, lineaments

and resultant structural features formed due to emplacement of diapiric granite. Therefore conventionally, geophysical strategies for diamond exploration have primarily consisted of delineation of intersecting lineaments and confined geophysical anomalies (Ramachandran et al. 1999, Nayak et al. 1999, Sharma et al. 1999).

Moreover it is known that mantle upwarp areas, linear crustal faults, granitic bodies recognizable on the ground by domal structures and zones of intersection of several trends are favorable locations for kimberlite emplacement (Subrahmanyam et al. 2006). Nayak et al. (2008) opined that the emplacement of kimberlites in the Dharwarcraton was triggered by the reactivation of major ENE-WSW trending faults approximately 1,100 million years age. Further, the regions of intersection of these faults with NW-SE trending faults formed the most likely zones for kimberlite localization.

Quantitative analysis of aeromagnetic analysis like Euler deconvolution depth solutions for pipes. Radially averaged Power spectrum depth profiles and GM- sys modeling and prognosticated kimberlite depth profiles were matched to concluded the prognosticated kimberlite locations and magnetic interface. Twenty21 new kimberlite locations and magnetic interface are prognosticated at the intersection of magnetic lineaments, which might be deep seated faults.

A map showing the distribution of magnetic sources and structural elements interpreted using the aeromagnetic anomalies and its various transformations its represented in Fig. 2. Magnetic sources were picked from the analytical signal map, while the tectonic elements were interpreted from a combination of the RTpmap and derivative map(horizontalX and Ydirection and first vertical derivative) map(Reeves (1985) and Wellman 1985) .

From a combination of RTP map (Fig.3) and its transformations the region in the area is characterized by essentially NW-SE trends in the northern part of study area changing completely to NE-SW in the southern part. The eastern part has higher concentrations of magnetic sources falling under Maddurkimberlite clusters.

The location where the trend changes from NW- SE to NE-SW canbe considered as the structural boundary. Another important features is the absence of NW-SE trends in the region south ofMaddur trend is ENE-WSW.

A clear change in trend from NW-SE to NE-SW can be noticed as one moves from west of Maddur region.

Conclusions

Through aeromagnetic studies and its subsurface lineaments (faults) support the emplacement of kimberlites at twenty one new locations in the study area. But all these kimberlites are concealed under the soil/regolith and available deep seated approximately about 400 -1200 mtr.

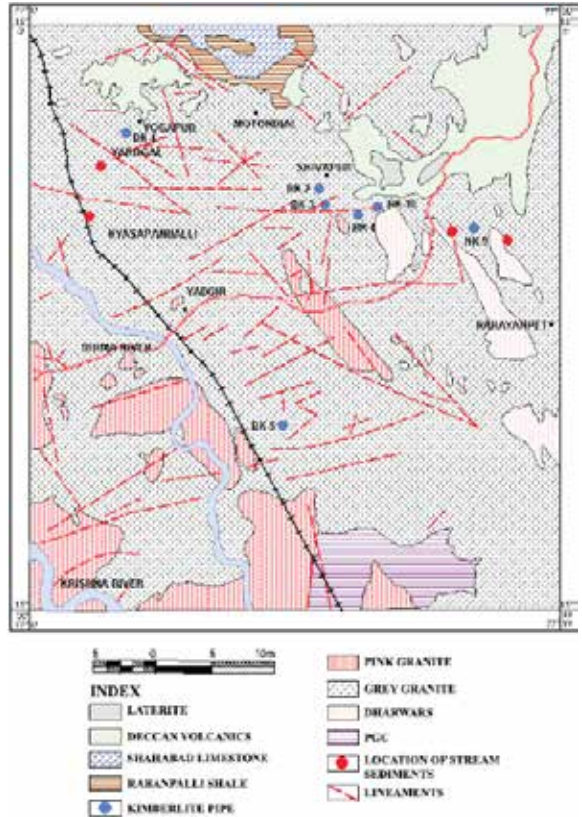


Figure 1.: Geological Map showing Narayanpet Kimberlite Field (NKF) (after GSI, 2011).

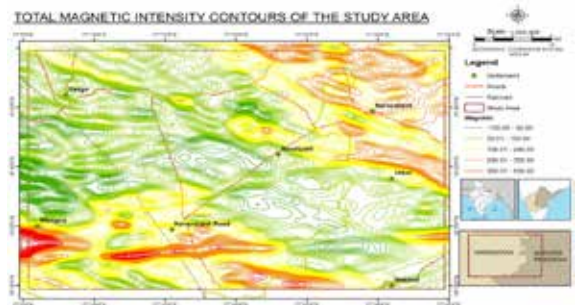


Figure2.: Total Magnetic Intensity (TMI) contours of the Study area.

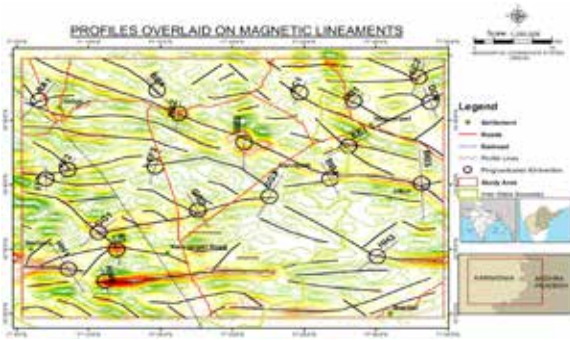


Figure 3.: Profiles overlaid on magnetic lineaments. B

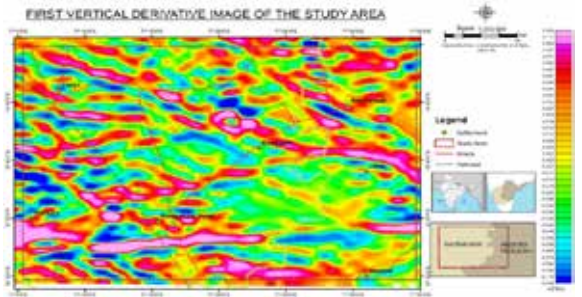


Figure. 7. First Vertical Derivative Image of the study area.

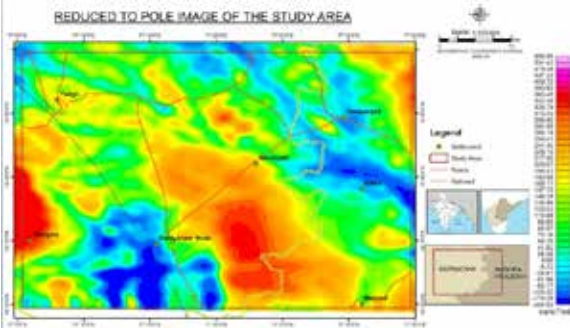


Figure.4.:Reduced to pole image of the Study area.

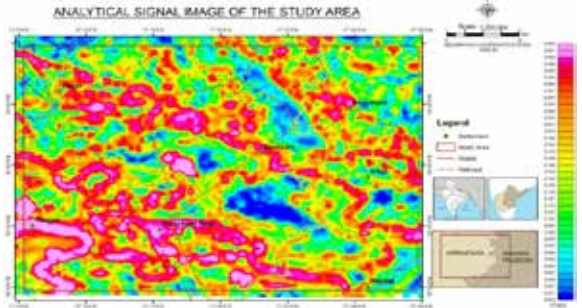


Figure.8. Analytical signal image of the study area.

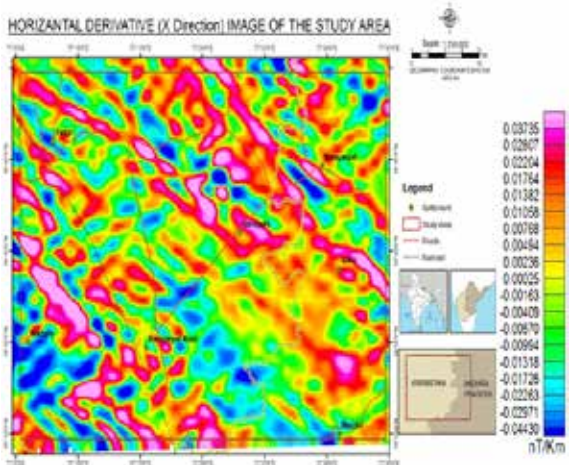


Figure 5.: Horizontal Derivative (X Direction) Map of the Study Area

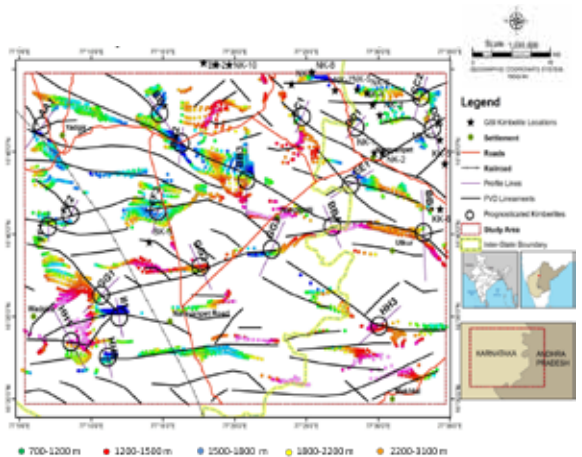


Figure.9. Prognosticated Kimberlite locations overlaid on magnetic lineaments, Euler depth solutions (points shown as fill-colored circles) and profile lines.

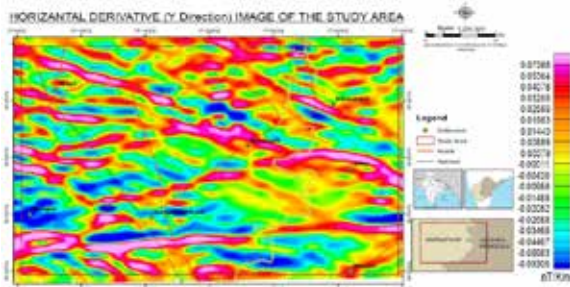
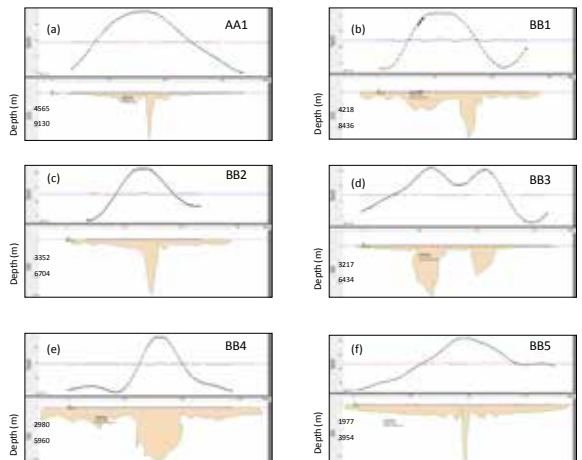


Figure.6.: Horizontal Derivative (Y Direction) Map of the Study Area.



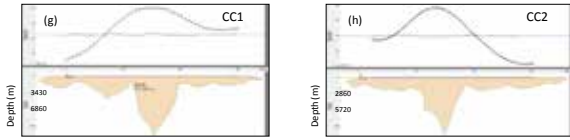


Figure.10.1. Inferred Magnetic Interface along profiles (a) AA1 (b) BB1 (c) BB2 (d) BB3 (e) BB4 (f) BB5 (g) CC1 (h) CC2

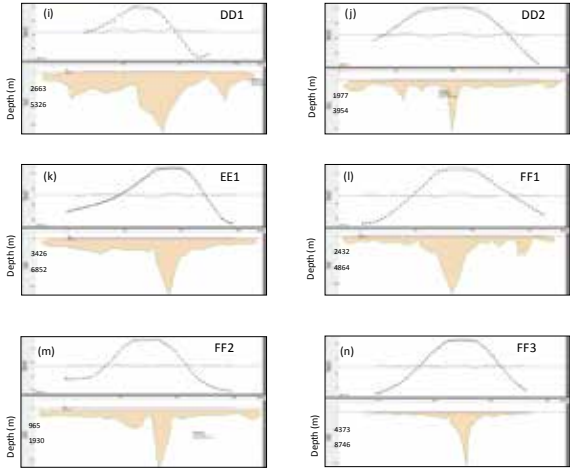


Figure.10.2. Inferred Magnetic Interface along profiles (i) DD1 (j) DD2 (k) EE1 (l) FF1 (m) FF2 (n) FF3

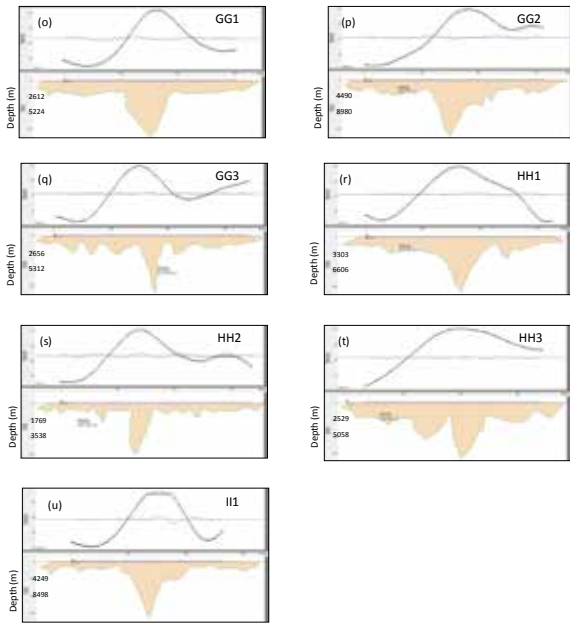


Figure.10.3.: Inferred Magnetic Interface along profiles (o) GG1 (p)GG2 (q) GG3 (r) HH1 (s) HH2 (t) HH3 (u) II1

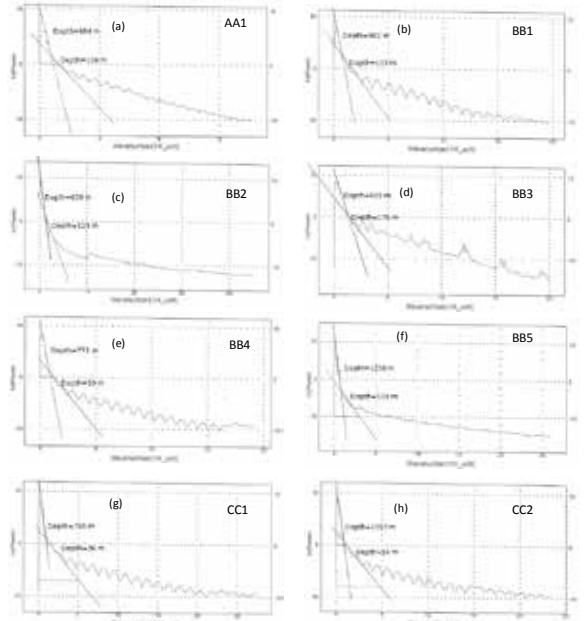


Figure.11.1.: Radially Averaged Power Spectrum of Profiles. (a) AA1 (b) BB1 (c) BB2 (d) BB3 (e) BB4 (f) BB5 (g) CC1 (h) CC2

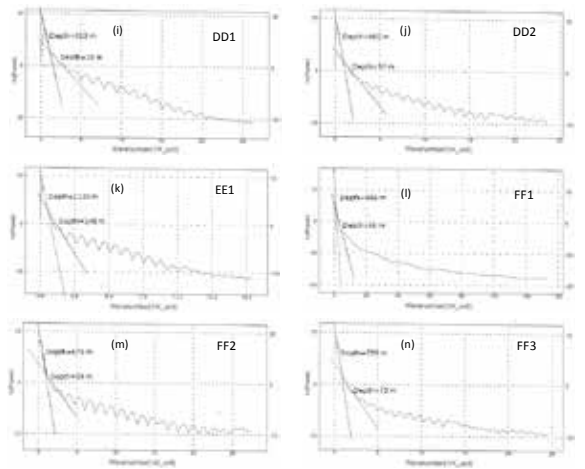
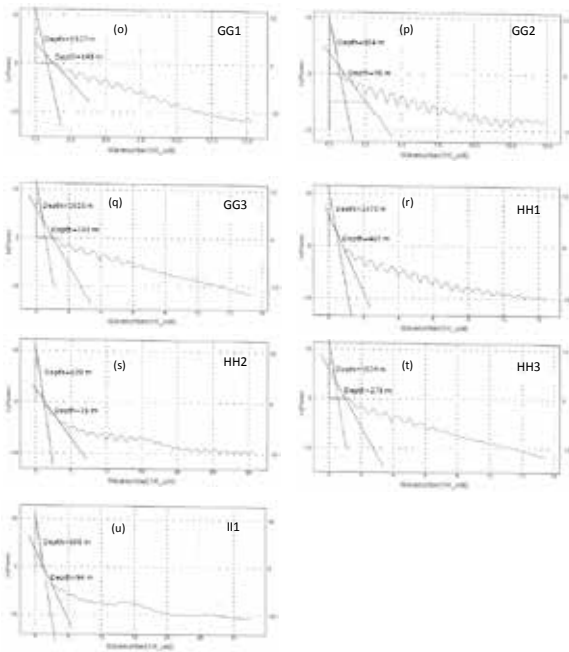


Figure.11.2.: Radially Averaged Power Spectrum of Profiles. (i) DD1 (j) DD2 (k) EE1 (l) FF1 (m) FF2 (n) FF3



Acknowledgement

The authors are grateful to the University Grants Commission (UGC), Govt. of India-New Delhi, for the sanctioning the Emeritus Fellowship of Prof.G. Ramadass and Dean development, Osmania University.

Figure.11.3.: Radially Averaged Power Spectrum of Profiles. (o) GG1 (p)GG2 (q) GG3 (r) HH1 (s) HH2 (t) HH3 (u) II1

Table –I

S. No.	Location of the Magnetic Body (Center Coordinate)		Profile	Peter's Half Slope Average Depths in meters	Euler De-convolution Depths in meters	Power Spetrum Depth(m)		Magnetic Interface depth in meters
	Longitude	Latitude				Magnetic 1 st interface	Magnetic 11 nd interface	
1	77°06'33.48"E	16°46'32.52"N	AA1	759	759	106	664	12,989
2	77°14'45.96"E	16°47'19.68"N	BB1	736	736	119	802	10,699
3	77°16'16.68"E	16°45'31.68"N	BB2	685	685	123	609	10,070
4	77°20'49.92"E	16°43'16.32"N	BB3	699	699	178	505	3,330
5	77°26'47.40"E	16°40'27.48"N	BB4	855	855	90	772	13,379
6	77°33'09.36"E	16°40'05.52"N	BB5	1640	1640	118	1338	8,702
7	77°24'41.76"E	16°47'07.80"N	CC1	738	738	36	755	9,727
8	77°32'57.84"E	16°48'20.16"N	CC2	1073	1073	54	1057	8,881
9	77°28'26.04"E	16°46'29.28"N	DD1	549	549	18	410	12,214
10	77°33'45.72"E	16°46'23.88"N	DD2	608	608	57	660	9,068
11	77°28'05.52"E	16°42'59.76"N	EE1	1223	1223	248	1130	11,850
12	77°07'01.20"E	16°40'27.48"N	FF1	699	699	40	586	10,049
13	77°08'33.72"E	16°41'10.32"N	FF2	765	765	39	675	8,132
14	77°14'39.12"E	16°41'24.36"N	FF3	768	768	73	755	6,683
15	77°10'41.52"E	16°36'18.36"N	GG1	911	911	145	1107	15,306
16	77°17'35.88"E	16°38'01.32"N	GG2	1061	1061	95	954	9,122
17	77°22'34.68"E	16°39'05.04"N	GG3	921	921	160	1016	8,401
18	77°08'35.52"E	16°33'28.44"N	HH1	1220	1220	467	1470	9,166
19	77°11'08.88"E	16°32'31.92"N	HH2	648	648	31	639	14,103
20	77°30'04.32"E	16°34'26.40"N	HH3	1631	1631	271	1534	5,192
21	77°11'57.12"E	16°34'58.44"N	II1	538	538	94	609	10,957

REFERENCE

- Balakrishna S, Rajamani V and Hanson G.N. 1999. U-Pb ages for zircon and titanite from the Ramagiri area, southern India: evidence for the accretionary origin of the eastern Dharwar craton during the late Archaean. | Babu Rao, V., Bijendra Singh and Jain, S.C. 1992. Geophysical exploration for kimberlites in Andhra Pradesh, India - A retrospect. *Jour. Assoc. Explor. Geophys.*, Vol. 13, pp. 15-22. | Baranov, V. 1957. A new method for interpretation of aeromagnetic maps pseudo-gravimetric anomalies. *Geophysics*. Vol. 22, pp. 359-383. | Baranov, V. and Naudy, H. 1964. Numerical calculation of the formula of reduction to the magnetic pole. *Geophysics*, Vol. 29, pp. 67-79. | Dobrin M.B and Savit C.H. 1988. Introduction to Geophysical Prospecting 4th Edition McGraw-Hill Book Co. pp. 667 | Haggerty, S.E. 1994. Superkimberlites: a geodynamic window to the Earth's core. *Earth Planet. Sci. Lett.* Vol. 122, pp. 57-69. | Haggerty, S.E. 1999. A diamond trilogy: superplumes, supercontinents, and supernovae. *Science* Vol. 285, pp. 851-860. | Janse, A.J.A. 1985. Kimberlites-where and when? In: Glover, J.E., Harris, P.G (Eds.). *Kimberlite Occurrence and Origin: A basis for Conceptual Models in Exploration*. University of Western Australia Special Publication. Vol. 8, pp. 19-61. | Janse, A.J.A. 1992. Archons and Cratons: Modern ideas on tectonic and structural control of economic kimberlites. *Proc. Int. Round Table Conf. on Diamond Exploration and Mining (26 & 27 Nov., New Delhi)*. | Krogstad E.J. Hanson G.N. Rajamani V. 1995. Sources of continental magmatism adjacent to the late Archaean Kolar suture zone, South India: distinct isotopic and elemental signatures of two late Archaean magmatic series. *Contrib. Miner. Petrol.* 122 pp 159-173. | Mitchell, R.H. 1986. *Kimberlites: Mineralogy, Geochemistry, and Petrology*. Plenum Press, New York. | Mitchell, R.H. 1991. Kimberlites and lamproites: primary sources of diamonds. *Geoscience Canada*, Vol. 18, pp 1-16. | Macnae, J.C. 1995. Applications of geophysics for detection and exploration of kimberlites and lamproites. *Journal of Geochemical Exploration*. Vol. 53 (1-3), pp. 213-243. Elsevier Science. | Mallick, K., Vasanthi, A. and Sharma, K.K. 2012. Bouguer Gravity Regional and Residual Separation: Application to Geology and Environment. Springer. | Nabighian, M.N., 1972. The analytic signal of two-dimensional magnetic bodies with polygonal cross-section—its properties and use for automated anomaly interpretation. *Geophysics*. Vol. 37, pp. 507-517. Nayak, S. S., Rao K, R. P., Kudari, S.A.D., Ravi, S., Kulashreshtha, S.K. and Bhaskar Rao, K.S. 1999. Search for kimberlites in the eastern block of the Dharwar craton: A Conceptual Model. *Journal of Geophysics, Special Issue*, Vol. 20, No. 4, pp. 195-204. | Nayak, S.S., Rao, K.R.P., Kudari, S.A.D. and Ravi, S. 2001. Geology and Tectonic setting of the Kimberlites and Lamproites of Southern India. National Seminar on Exploration and Survey for Noble Metals and Precious Stones. Special Publication No. 58. Geological Survey of India. pp. 567-575. | Nayak, S.S., Reddy, N.S. and Roopkumar, D. 2008. Petrological and Petrochemical Studies of the Kimberlites and their Xenoliths of Dharwar Craton. *Geological Survey of India Progress Report for the Field Seasons 2002-2003 and 2003-2004*. | Ramadass, G., Himabindu, D. and Ramaprasada Rao, I.B. 2004a. Magnetic basement along the Jadcharla-Vasco transect, Dharwar Craton, India. *Current Science*, Vol. 84, No. 11. | Ramadass, G., Himabindu, D. and Ramaprasada Rao, I.B. 2004b. Magnetic basement of the Dharwar Craton in the Precambrian Indian Peninsular Shield. *Current Science*, Vol. 86 (11), pp. 1548-1553. | Ramadass, G., Himabindu, D. and Veeraiah, B. 2006a. Morphostructural Prognostication of Kimberlites in parts of Eastern Dharwar Craton: Inferences from Remote Sensing and Gravity Signatures. *Journal of the Indian Society of Remote Sensing*, Vol. 34, No. 2, pp. 111-121 | Ramadass, G., Ramaprasada Rao, I.B. and Himabindu, D. 2006b. Crustal configuration of the Dharwar Craton, India, based on joint modeling of regional gravity and magnetic data. *Jour. Asian Earth Sci.*, Vol. 26, pp. 437-448. | Ramadass, G., Ramaprasada Rao, I.B. and Himabindu, D. 2007. Dharwar craton: crustal model from regional gravity and magnetic signatures. *Int. Assoc. Gondwana Res. (IAGR) Japan, IAGR Memoir*, No. 10, pp. 227-232. | Ramam, P.K., Murthy, V.N. 1997. Geology of Andhra Pradesh. Geological Society of India, Bangalore. | Rao, D.A. 1996. Intra-crustal structure inferred from aeromagnetics in a part of the Dharwar craton and its significance in kimberlite exploration. *Journal of the Geological Society of India*. Vol. 48, pp. 391-402. | Rajamani V. 1990. Petrogenesis of metabasites from the schist belts of the Dharwar Craton Implications in Archaean mafic magmatism. *Jour. Geol. Soc. India* Vol. 36 pp 565-587. | Ramachandran C Kesavamani M and Prasad R.M.C. 1999. A geophysical prognostication of primary diamond deposits in peninsular India. *Jour. Geophysics*. Vol. 20. No. 4 pp 155-178. | Spector, A. and Grant, F. 1970. Statistical models for interpreting aeromagnetic data. *Geophysical*. Vol. 35, pp. 293-302. Ramachandran, C., Kesavamani, M. and Prasad, R.M.C. 1999. A geophysical prognostication of primary diamond deposits in peninsular India. *Journal of Geophysics*, Vol. 20. No. 4, pp. 155-178. | Sharma, K.K., Rao, V.K. and Mallick, K. 1999. Finite element gravity regional and residual anomalies and structural fabrics of northwest Ganga basin. *Journal of the Geological Society of India*. Vol. 59. Pp. 169. | Sreerama Murthy, N., Ananda Reddy, R., Livingston, D., Raju, V.L. and Mohan Rao, T. 1997. Geophysical exploration of kimberlite pipes—a case study from Maddur area, Mahabubnagar district, Andhra Pradesh. *Journal of Geophysics*. Vol. 18, pp. 165-174. | Sreerama Murthy, N., Ananda Reddy, R., Rao, M.V.R.K., Sunder Raj, B., Murthy, N.V.S. and Vittal Rao, K.P.R. 1999. A new kimberlite discovery from a structural elucidation of gravity data, Maddur – Narayanpet field, Mahabubnagar district, Andhra Pradesh. *Journal of Geophysics*, Vol. 20, no. 1, pp. 3-13. | Sykes, L.R. 1978. Intraplate seismicity, reactivation of preexisting zone of weakness, alkaline magmatism and other tectonism postdated continental fragmentation. *Rev. Geophys. Space. Phys.* Vol. 16 (4), pp. 521-688. | Talwani, M., Worel, J.L. and Landisman, M. 1959. Rapid gravity computations for two-dimensional bodies with application to the Mendocino submarine fracture zone. *Journal of Geophysical Research*. Vol. 64, pp. 49-59. | Talwani, M. and Heirtzler, J.R. 1964. Computation of magnetic anomalies caused by two dimensional bodies of arbitrary shape, in Parks, G.A. Ed., *Computers in the mineral industries, Part 1*. Stanford University Publication. Geological Sciences. Vol. 9, pp. 464-480. | Veeraiah, B., Himabindu, D. and Ramadass, G. 2006. Geological and Structural Inferences from Satellite Image in Parts of the Eastern Dharwar Craton, India. *Journal of Indian Geophysical Union*, Vol. 10, No. 3, pp. 255-262. | Veeraiah, B., Ramadass, G. and Himabindu, D. 2009. A subsurface Criterion for Predictive Exploration of Kimberlites from Bouguer Gravity in the Eastern Dharwar Craton, India. *Journal of Geophysics of India*. Vol. 74, pp. 69-77. | Woodzick, T.L. and McCallum, M.E. 1984. A teledetective study of kimberlite regions in North America (Colorado-Wyoming), East Africa (Mwadu) and Siberia (Mir). *Kimberlites and Related Rocks*. pp. 5-20. | Webring M. 1985. SAKI. A Fortran program for generalized linear inversion of gravity and magnetic profiles. *USGS Open File Report*. Vol. 29, pp 85-122. | Won I.J and Bevis M. 1987. Computing the gravitational and magnetic anomalies due to a polygon. *Algorithms and Fortran subroutine*. *Geophysics*. Vol. 52, pp 232-238 | GSI. 2011. Detailed information Dossier on Diamond in India. Geological Survey of India. | Margaret, D.W. 1963. An algorithm for least squares estimation of non-linear parameters. *Journal of SIAM*. Vol. 11, pp. 431-441. | Power, M., Belcourt, G. and Rockel, E., 2004. Geophysical methods for kimberlite exploration in northern Canada. *The Leading Edge*, Vol. 23, No. 11, pp. 1124 – 1129. | Rao, K.R.P., Reddy, T.A.K., Rao, K.V.S., Rao, K.S.B. & Rao, N.V. 1998. Geology, petrology and geochemistry of Narayanpet kimberlite field in Andhra Pradesh and Karnataka. *Journal of the Geological Society of India*, Vol. 52, pp. 663-676. | Sinha, P.K., Surendranath, M., De, S.K., Muralidharan, P.K. and Misra, R.S. 2003. A GIS approach in Mineral Targeting with Narayanpet Kimberlite Spatial Dataset. *Map India Conference 2003*. | Subrahmanyam, V., Subrahmanyam, A.S., Kishor, K.S.R., Murthy, G.P.S., Sarma, K.V.L.N.S., Rani, P. Suneta. And Anuradha. A. 2006. Precambrian magmatic lineaments across the Indian sub-continent—preliminary evidence from offshore magnetic data. *Current Science*, Vol. 90, No. 4. |